Electronic Supporting Information

Contents

Experimental part

Reagents

All reagents and chemicals were purchased from commercial sources and used without additional purification. The following reagents were used as starting reagents: $EuCl_3 \cdot 6H_2O$ (powder), KOH (powder), H_2nda_3 (powder), H_2tph_3 (powder), *o*-phenotroline (powder), Bphen (powder).

Analysis methods, equipment and technical details of experiments

The IR spectra of the complexes were recorded using a Perkin Elmer SpectrumOne FTIR spectrometer in the range 350-7800 cm^{-1}.

Thermal analysis (TA) was performed on a NETZSCH STA 409 PC Luxx thermal analyzer (NETZSCH, Germany) at a heating rate of 10 °C/min (sample weight 5-10 mg). The composition of the gas phase formed during decomposition of the samples was studied using a quadrupole mass spectrometer QMS 403C Aeolos (NETZSCH, Germany) combined with a thermal analyzer NETZSCH STA 409 PC Luxx. Mass spectra were recorded for the mass numbers 18 (H_2O), 44 (CO_2) and 58 (acetone).

Single crystal X-ray diffraction. Single crystal diffraction experiments were carried out using a Bruker APEX Duo CCD diffractometer (ω scans) at 120K using Cu-Ka and Mo-Ka radiation. All calculations were performed using the SHELX program version 2014/6.

Powder diffraction of PXRD. The powder patterns of the studied compounds were measured using a Bruker D8 Advance Vario diffractometer with Ge(111) using a monochromator in the transmission mode between polyester films (Mylar), as well as on a Bruker D8 Advance diffractometer in reflection mode using a silicon stand (Bragg-Brentano geometry, with variable slits). Both diffractometers are equipped with a LynxEye 1D detector. And also on the RIGAKU smartLAB diffractometer in the range 2-60º. Indexing was performed using the SVD [45] algorithm in the TOPAS 4.2 program [46].

Photoluminescence spectra and excitation spectra were measured on a Fluoromax spectrofluorometer using a xenon lamp with tunable wavelength as an excitation source. All luminescence and excitation spectra were removed with an adjustment for instrumental functions. The excitation spectra were recorded at a wavelength of 612 nm.

The radiative lifetime of the excited state was also calculated for X europium:

$$\frac{1}{\tau_{rad}} = 14{,}65 \times n^3 \times \left(\frac{I_{tot}}{I_{MD}}\right) \qquad (3)$$

The excitation spectra were measured at the wavelength of luminescence of the central REE ion. The bands in them correspond to the absorption of ligands, which is then transferred to the REE ion by intramolecular transfers and emitted as a quantum of light. By the appearance of additional bands in the excitation spectrum, it is possible to judge the coordination of additional ligands that are also involved in the sensitization of the luminescence of the REE ion. A decrease in the intensity of any excitation band indicates the appearance of additional processes competing with the luminescence of the REE ion, such as reverse energy transfer, sensitization of the luminescence of an organic ligand or nonradiative relaxation of the excited state, which usually also indicates the formation of a new compound.

The lifetime of the excited state was determined using a Fluoromax spectrofluorometer. This value is a luminescent characteristic sensitive to the coordination environment and is determined from the luminescence attenuation curves according to equation (4):

$$y = y_o + B\ exp\left(-\frac{t}{\tau}\right) \qquad (4)$$

where y is the measured luminescence intensity at time t after the laser pulse, B is the luminescence intensity at time t=0, τ=τ_obs is the lifetime of the excited state, or the decay time of luminescence, y0 is the consideration of the background signal.

The lifetime depends on the constants of the radiative (krad) and nonradiative (knr) processes of deactivation of the excited state of the REE ion:

$$\tau_{obs} = \frac{1}{k_{rad}+k_{nr}} \qquad (5)$$

The radiative lifetime can be calculated for X europium, using these data it is possible to calculate the internal quantum yield Q_Ln^Ln, that is, the quantum yield when excited through a ligand:

$$Q_{Ln}^{Ln} = \frac{\tau_{obs}}{\tau_{rad}} \qquad (6)$$

By the nature of the luminescence quenching curve after a single excitation, namely, by whether the quenching curve is described mono-, bi- or polyexponential dependence, it is possible to judge the formation of an individual compound in the case of monoexponential dependence or a mixture of compounds in other cases. A change in the lifetime of the excited state indicates a change in the coordination environment of the REE ion, which usually indicates the formation of a new compound: coordination of an additional ligand, ligand exchange, etc.

All luminescent characteristics are quite sensitive and therefore theoretically can differ not only when comparing different compounds or one compound in the form of powder and solution, but also when switching from powder to thin film. When comparing the luminescent characteristics of a compound in the form of a powder and a thin film, it is possible to judge whether the composition matches or does not match.

The quantum yields of the powders were measured at room temperature when excited through a ligand to characterize the luminescence efficiency. Measurements were performed on a Fluoromaxm spectrofluorometer using an integrating sphere.

Synthesis

Synthesis of homogeneous ligand complexes

The synthesis of $Eu_2(L)_3(H_2O)_x$ (HL = H_2nda, H_2tph) was carried out in an aqueous, aqueous-organic or organic medium by reacting a solution of $EuCl_3$•$6H_2O$ with a solution of potassium salt of the corresponding acid obtained in situ by neutralization of the acid with an alkali solution, in a molar ratio of 3:2.

Synthesis of mixed-ligand complexes

Synthesis of $Eu_2(carb)_3(Q)(H_2O)_x$ complexes (carb = H_2nda, H_2tph; Q = Phen, Bphen) was performed by reacting solutions of the corresponding $EuCl_3(Q)_2$×H2O obtained in situ by the reaction of lanthanide chloride with a neutral ligand solution, with an excess of the corresponding potassium carboxylate obtained in situ by the interaction of KOH and the corresponding acid. The sediment of the multi-ligand complex was separated by filtration and dried in air.

$Eu_2(nda)_3(BPhen)_2(H_2O)_4$ single crystal

A mixture of H_2nda (0.0432 g, 0.2 mol), Bphen (0.0665 g,0.2 mmol), 0.1 mmol KOH (0.0336 g), 0.1 mmol $EuCl_3$•$6H_2O$ (0.0732 g) and water (20 ml) was placed in a sealed 50 ml stainless steel reactor with Teflon lining and heated at 180°C for 72 hours, then brought to 100 °C for 24 hours and kept at 100 °C for 24 hours, then slowly cooled to room temperature.

A suitable crystal was selected and mounted using glass fiber on a Bruker APEX-II CCD diffractometer. The crystal was kept at 120 K during data collection. Using Olex2 [1], the structure was solved with the SHELXT [2] structure solution program using Intrinsic Phasing and refined with the XL [3] refinement package using Least Squares minimisation.

1. Dolomanov, O.V., Bourhis, L.J., Gildea, R.J, Howard, J.A.K. & Puschmann, H. (2009), J. Appl. Cryst. 42, 339-341.
2. Sheldrick, G.M. (2015). Acta Cryst. A71, 3-8.
3. Sheldrick, G.M. (2008). Acta Cryst. A64, 112-122.

Crystal structure

Crystal Data for $C_{42}H_{29}EuN_2O_8$ (*M* =841.63 g/mol): triclinic, space group P-1 (no. 2), *a* = 9.0051(3) Å, *b* = 11.6133(3) Å, *c* = 17.4351(5) Å, *α* = 72.3670(10)°, *β* = 81.1620(10)°, *γ* = 82.4180(10)°, *V* = 1709.97(9) Å^3, *Z* = 2, *T* = 120 K, μ(MoKα) = 1.895 mm^{-1}, *Dcalc* = 1.635 g/cm^3, 21560 reflections measured (2.468° ≤ 2Θ ≤ 61.212°), 10223 unique (R_{int} = 0.0310, R_{sigma} = 0.0574) which were used in all calculations. The final R_1 was 0.0291 (I > 2σ(I)) and wR_2 was 0.0574 (all data).

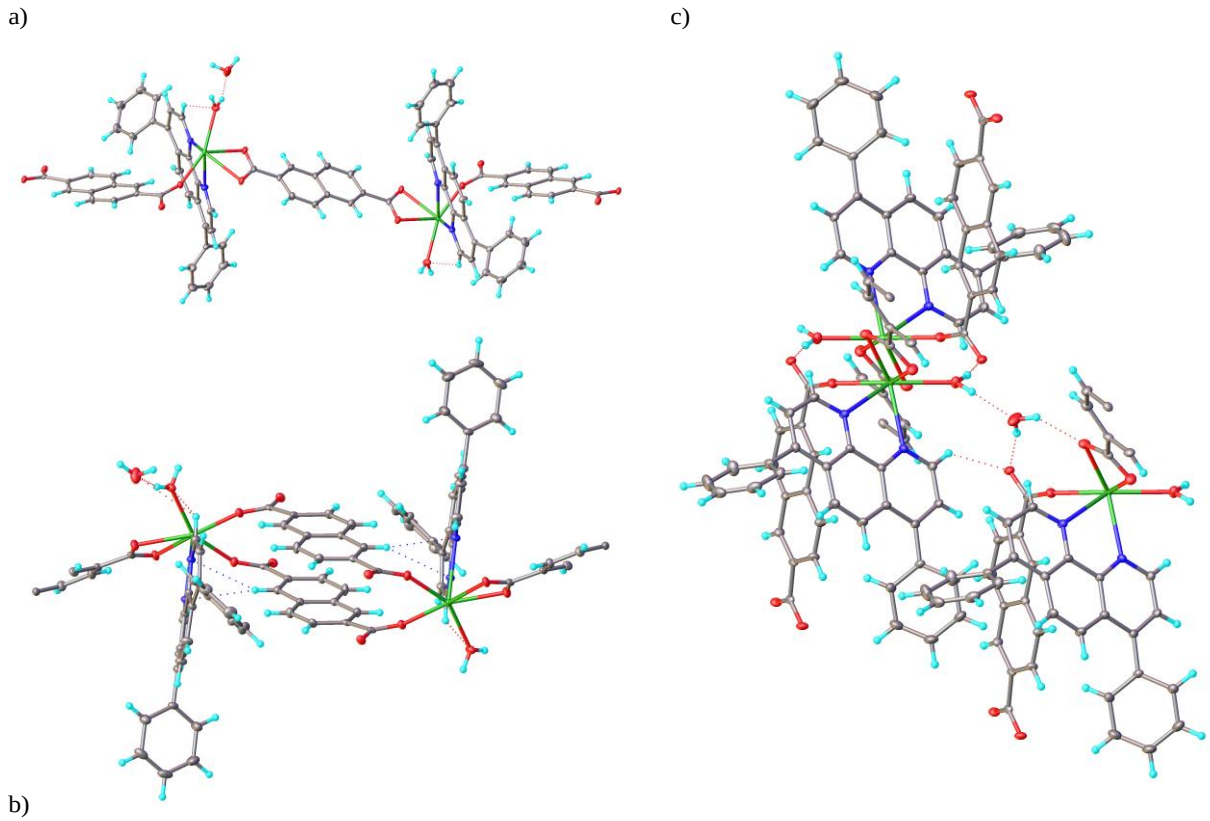

Fig. S1 a) $Eu_2(nda)_3(BPhen)(H_2O)_4$ cell, the centrosymmetric dimed bonded via nda ligand. b) The bonding motif and stacking of the second nda ligand. c) Hydrogen bonds in the crystal.

PXRD data

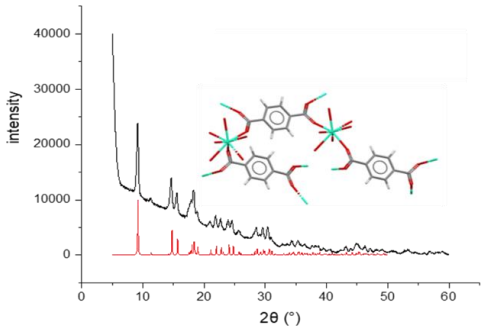

a)

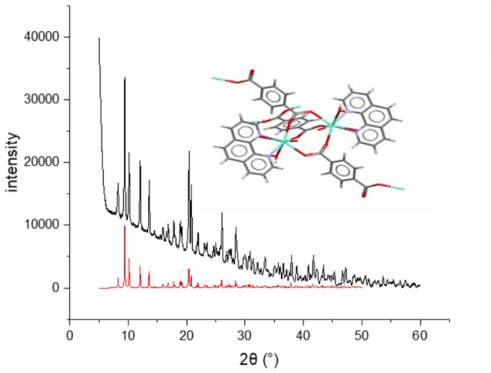

b)

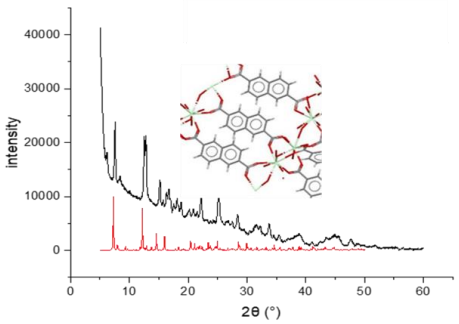

c)

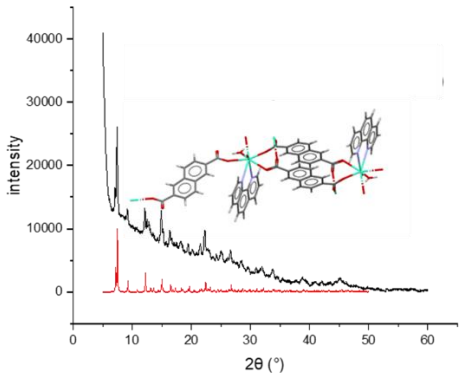

d)

Fig. S2 PXRD patterns of a) $Eu_2(tph)_3(H_2O)_4$, b) $Eu_2(tph)_3(phen)_2(H_2O)_4$, c) $Eu_2(nda)_3(H_2O)_4$, d) $Eu_2(nda)_3(phen)_2(H_2O)_4$

TGA data

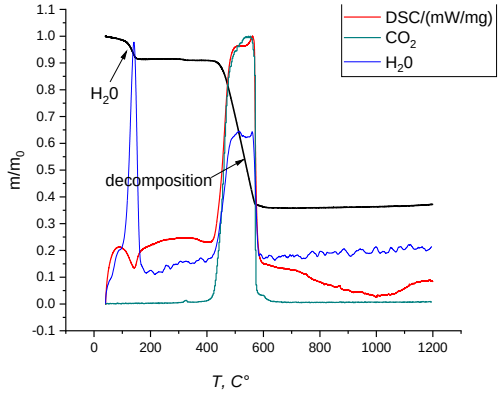

a)

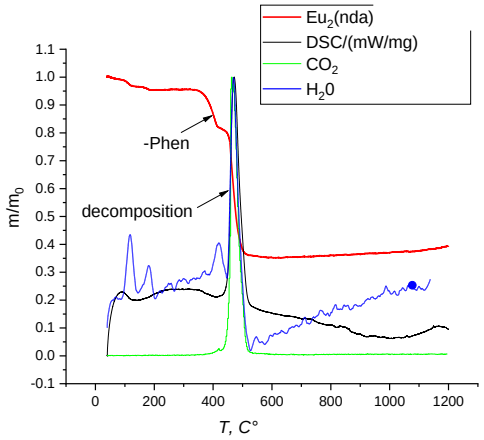

b)

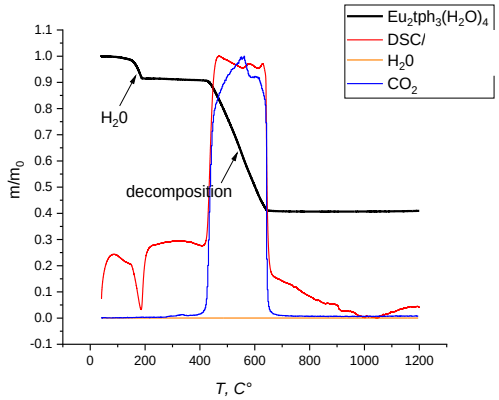

c)

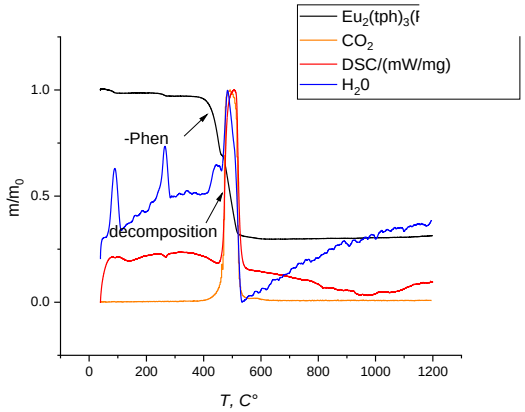

d)

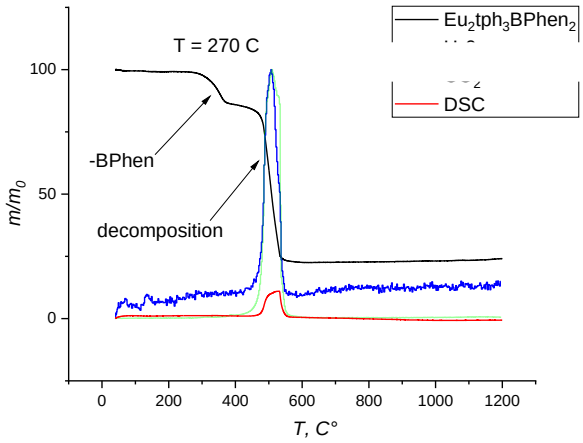

e)

Fig. S3 TGA data: a) $Eu_2(nda)_3(H_2O)_4$, b) $Eu_2(nda)_3(Phen)_2(H_2O)_4$, c) $Eu_2(tph)_3(H_2O)_4$, d) $Eu_2(tph)_3(Phen)_2 \cdot 4H_2O$, e) $Eu_2(tph)_3BPhen_2$

Photoluminescence

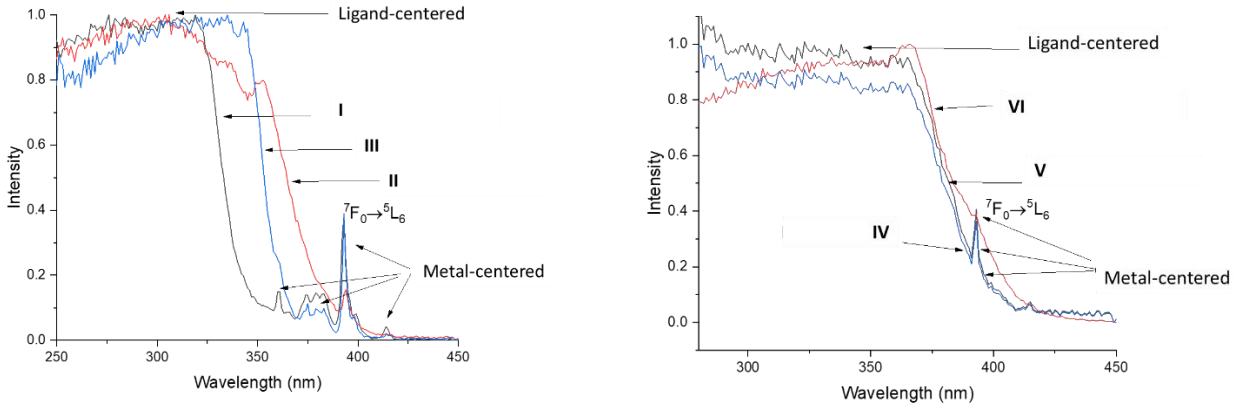

Fig. S4 PLE spectra of complexes

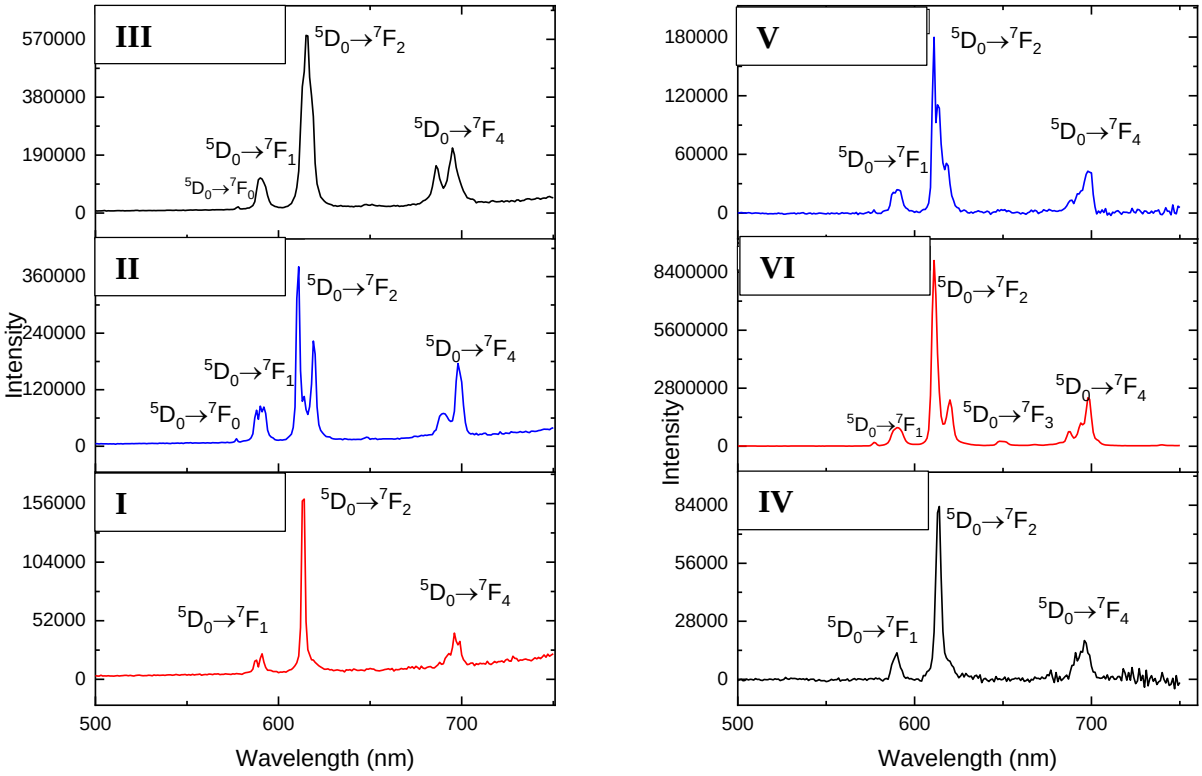

Fig. S5 PL spectra of complexes

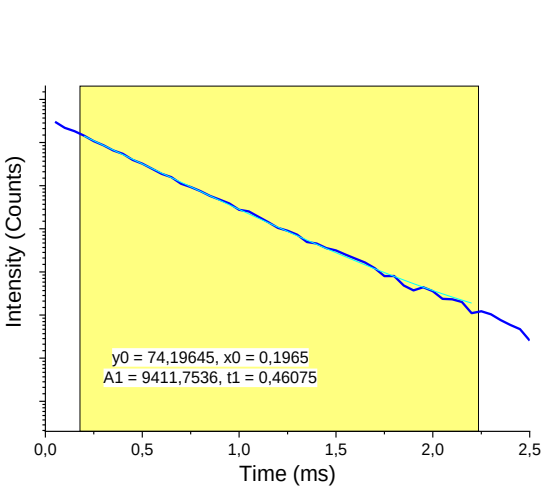
Intensity (Counts)
y0 = 74,19645, x0 = 0,1965
A1 = 9411,7536, t1 = 0,46075
0,0
0,5
1,0
1,5
2,0
2,5
Time (ms)

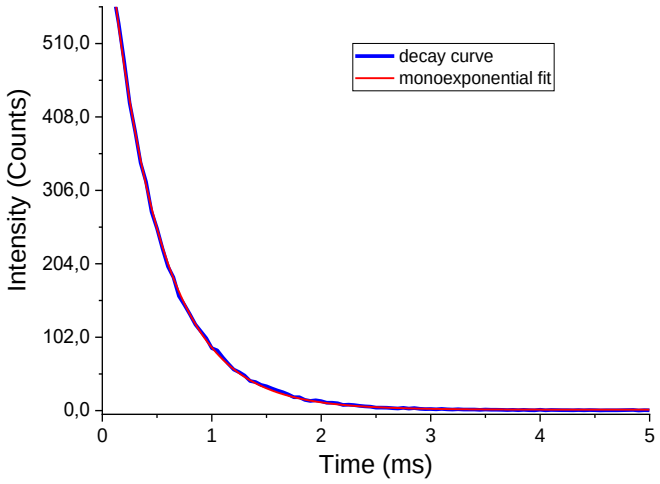
decay curve
monoexponential fit
Intensity (Counts)
510,0
408,0
306,0
204,0
102,0
0,0
0
1
2
3
4
5
Time (ms)

a)

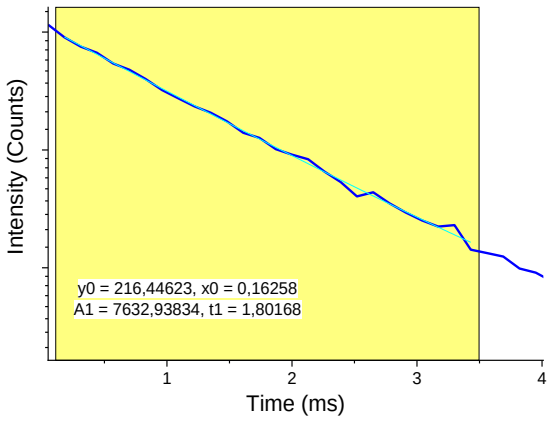
Intensity (Counts)
y0 = 216,44623, x0 = 0,16258
A1 = 7632,93834, t1 = 1,80168
1
2
3
4
Time (ms)

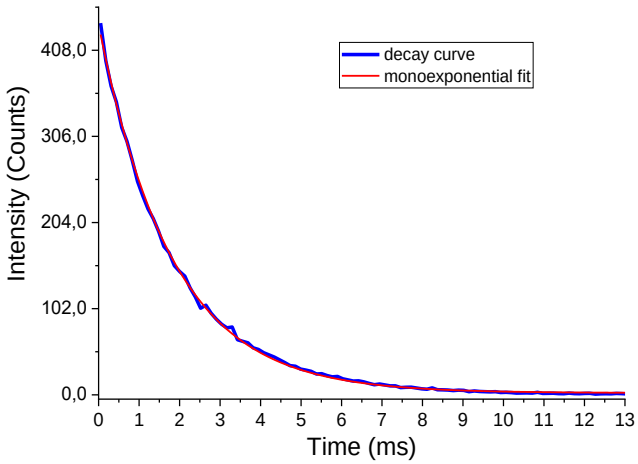
decay curve
monoexponential fit
Intensity (Counts)
408,0
306,0
204,0
102,0
0,0
0
1
2
3
4
5
6
7
8
9
10
11
12
13
Time (ms)

b)

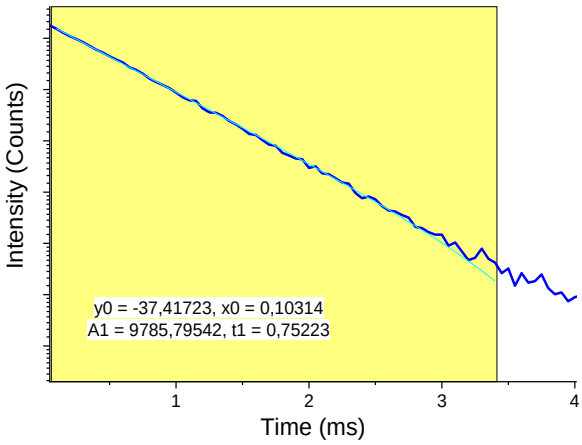
Intensity (Counts)
y0 = -37,41723, x0 = 0,10314
A1 = 9785,79542, t1 = 0,75223
1
2
3
4
Time (ms)

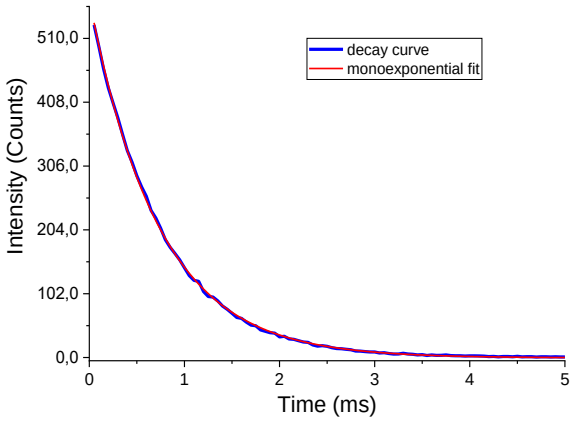
decay curve
monoexponential fit
Intensity (Counts)
510,0
408,0
306,0
204,0
102,0
0,0
0
1
2
3
4
5
Time (ms)

c)

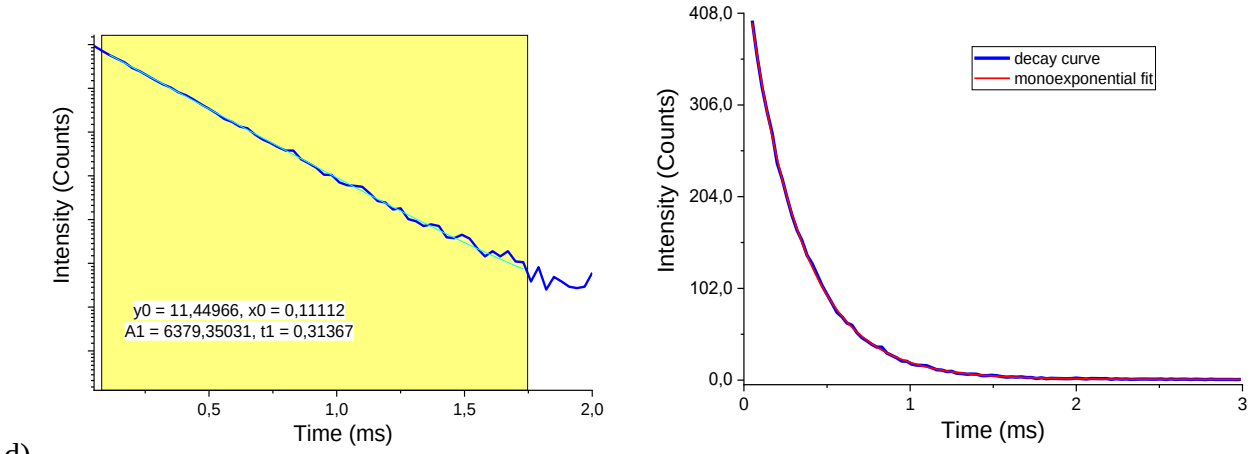

d)

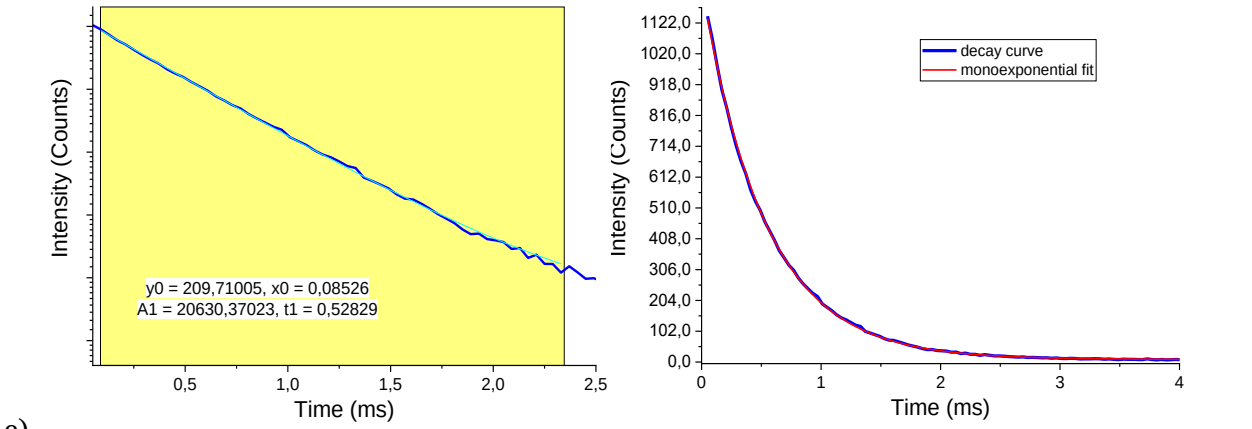

e)

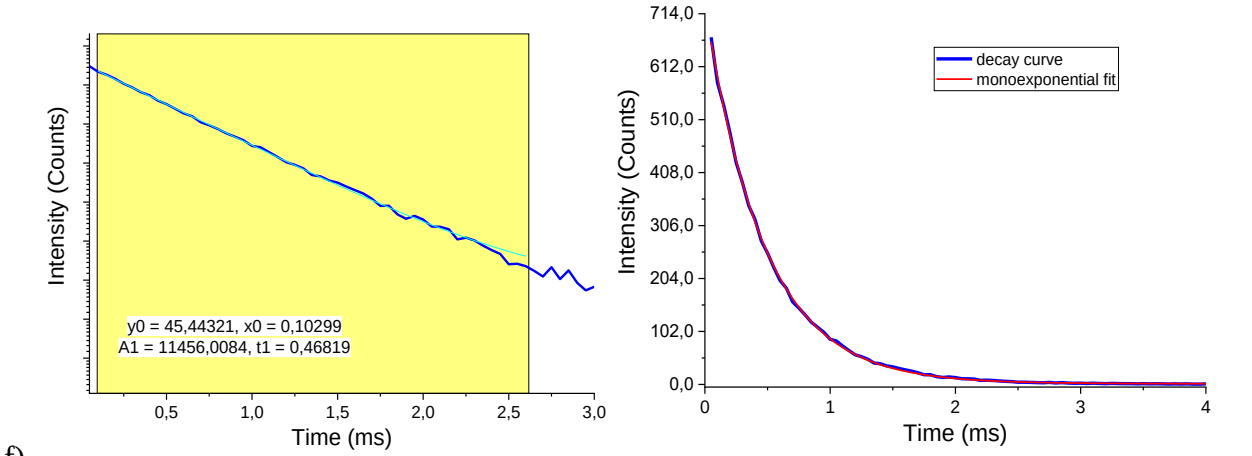

f)

Fig. S6 Luminescence decay curves of complexes: a) **I**, b) **II**, c) **III**, d) **IV**, e) **V**, f) **VI**. Excitation wavelength 280 nm. Left: semi-logarithmic scale. Right: linear scale.

Cathodoluminescence

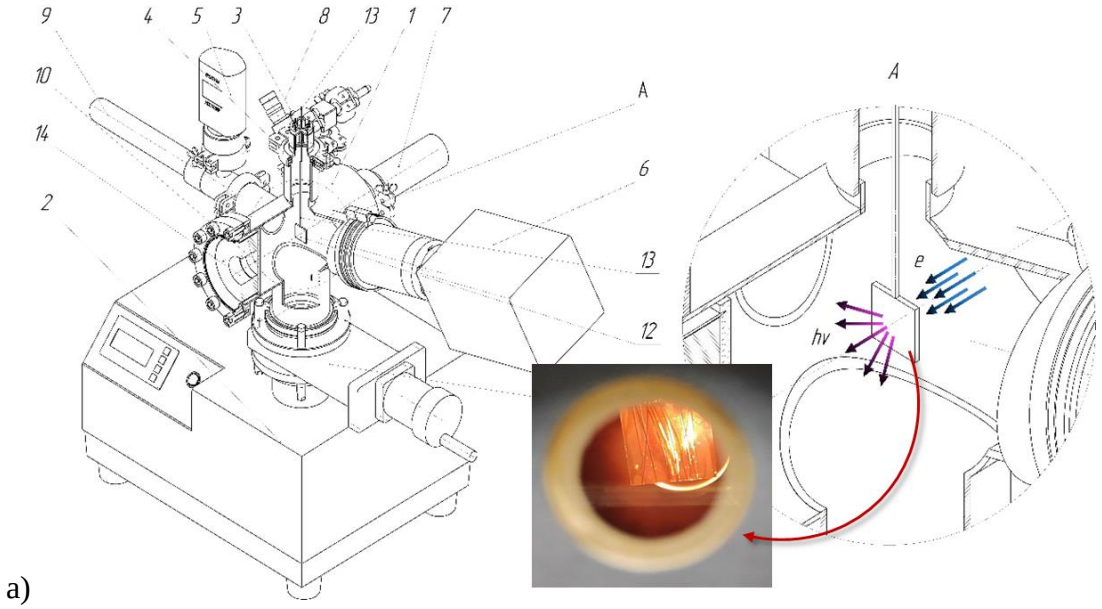

a)

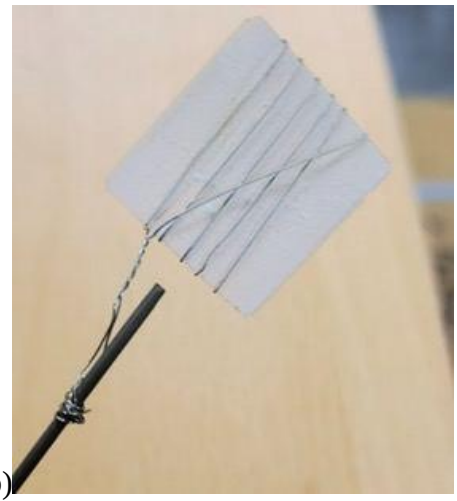

b)

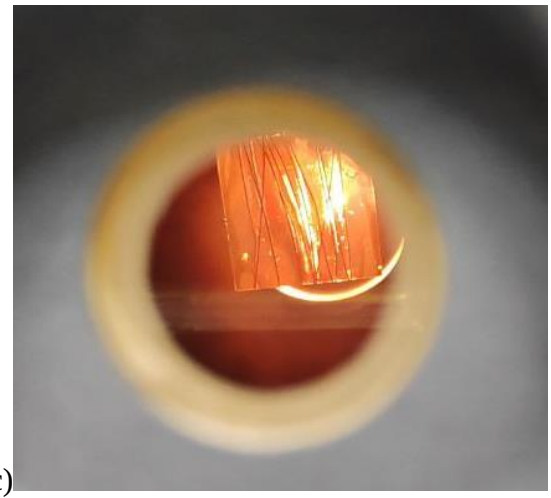

c)

Fig. S7 a) Laboratory vacuum system for determining the output characteristics of cathode phosphors.

b) The sample wrapped with the aluminum wire. c) The same sample inside of the device, the view through the window under the fast electron flow.

It consists of an analytical vacuum chamber (1) connected to an oil-free pumping system (2). On the chamber there are: a high-voltage sealed electrical input for connecting the traverse of the substrate holder (3) located on the loading flange (4), a wide-range vacuum sensor (5), a quadrupole mass spectrometer (6), cathode ray gun (7), gas leak (8), quartz tube (9), quartz exit

window (10), high vacuum slide gate (11). The head of the optical radiation power meter or the waveguide of the optical spectrometer is connected to the output quartz window (10).

The principle of the experiment is as follows. The quartz substrate (12), pre-matted on one side, is coated with a cathodoluminophore from an alcohol suspension, dried in a vacuum drying cabinet at a temperature of 100 ° C installed in an analytical chamber parallel to the output quartz window on the substrate holder. Before installation in the camera, an electrically conductive layer is applied to the phosphor or a parallel mesh is wound in increments of no more than 2 mm. The system is pre-pumped by a vacuum pump to a pressure not higher than $1 \cdot 10^{-2}$ Torr, then a high-vacuum turbomolecular pump is turned on and pumped to a pressure not higher than $5 \cdot 10^{-7}$ Torr. After thermodynamic equilibrium is reached, the power is turned on in the analytical chamber (not shown in the figure). An incandescent voltage is applied to the cathode of the electron beam gun. The operating temperature of the cathode W is in the range – 2400÷2600°C, the cathode efficiency is 2÷10 mA/W. To achieve the set temperature range, the glow voltage is set in the range of 2-4 V. The accelerating electrode of the electron beam gun is supplied with a voltage in the range of 100-200 V. The accelerating electrode is necessary to increase the kinetic energy of the thermoelectrons and allows focusing the flow of electrons into the beam. The modulating electrode of the electron beam gun is under the negative potential of the cathode. A positive potential in the range from 2 to 10 kV is supplied to the high-voltage input (13) connected to the traverse of the substrate holder. After registering the glow of the cathodoluminophore, the optimal parameters of the incandescent lamp and the anode voltage are selected, at which the brightness of the sample will be maximum. To measure the brightness, an optical head corresponding to the radiation range of the cathodoluminophore sample is attached to the radiometer. The optical head is installed in the socket (14) of the output quartz window (10). The power of optical radiation is measured in W/m^2.

To register the radiation spectrum, the waveguide of an optical spectrometer (MayaPro, Ocean Optics) is connected to the output quartz window (10).

After the study is completed, the incandescent voltage, the accelerating electrode voltage and the high anode voltage are switched off. The high vacuum slide gate is blocked, and a gas leak opens. After equalizing the pressure in the chamber with the atmosphere, the loading flange is opened and the test sample is replaced.